BULLETIN OF THE POLISH ACADEMY OF SCIENCES
TECHNICAL SCIENCES, Vol. 72(4), 2024, Article number: e149177
DOI: 10.24425/bpasts.2024.149177

Selection of reference model for adaptive PMSM drive based on MRAC approach

Rafal SZCZEPANSKI[1]*, **Tomasz TARCZEWSKI**[1], and **Lech M. GRZESIAK**[2]

[1] Department of Automatics and Measurement Systems, Nicolaus Copernicus University, Grudziadzka 5, 87-100 Torun, Poland
[2] Institute of Control and Industrial Electronics, Warsaw University of Technology, Koszykowa 75, 00-662 Warsaw, Poland

Abstract. The selection of a reference model (RM) for a Model-Reference Adaptive Control is one of the most important aspects of the synthesis process of the adaptive control system. In this paper, the four different implementations of RM are developed and investigated in an adaptive PMSM drive with variable moment of inertia. Adaptation mechanisms are based on the Widrow-Hoff rule (W-H) and the Adaptation Procedure for Optimization Algorithms (APOA). Inadequate order or inaccurate approximation of RM for the W-H rule may provide poor behavior and oscillations. The results prove that APOA is robust against an improper selection of RM and provides high-performance PMSM drive operation.

Keywords: PMSM drive; model-reference adaptive control; Widrow-Hoff rule; Adaptation Procedure for Optimization Algorithms.

1. INTRODUCTION

An adaptive controller allows modification of the controller coefficients in the case of a plant parameters change or external disturbance. As a result, superior dynamics, regardless of the system operating point, can be obtained. Adaptive controllers are commonly used to compensate for non-linearities [1, 2], electrical parameters variations [3], keep the highest possible performance [4], or ensure constant dynamics regardless of dynamics fluctuation [5, 6]. In this proposal, the latter issue is considered. One of the most commonly used adaptive control approaches to solving the analyzed problem is model-reference adaptive control (MRAC). Its goal is to keep the same system response regardless of plant parameter variation and external disturbances [7]. The reference model has to be defined as a desired system response in this approach. Next, the adjustment mechanism responsible for minimizing the difference between the reference model response and the system one is introduced. The convergence between the reference model and the system is obtained by modifying the controller coefficients. It should be noted that the system highest possible performance is typically not considered in the MRAC approach.

To ensure the perfect tracking of the reference model, in the case of plant parameters fluctuation, the plant (i.e., electrical drive in this particular case) should operate within a linear range for a considered span of parameter fluctuations (i.e., without limitation of state variables). It is crucial since an increased moment of inertia requires higher electromagnetic torque to maintain the same rising time of step response [8]. The latest applications of the MRAC approach are (i) motor control of autonomous ground vehicles [9], (ii) scalar control scheme with high starting torque for induction motors [10], (iii) velocity control of conveyor belt system [11], (iv) active damping of driveline vibration in power-split hybrid vehicles [12], (v) control of twin-rotor helicopter configuration [13], to name a few.

Several control structures can be utilized in the PMSM drive based on the MRAC approach. In [14], a typical cascade-control structure with non-adaptive PI current controllers and adaptive PI speed controller is applied. The initial values of the controller coefficients can be obtained using well-known tuning methods. However, poor load torque compensation is the main disadvantage of this solution. In [15], a hybrid solution with cascade control structure with PI speed and current controllers augmented by the linear quadratic adaptive regulator for IPMSM is proposed. The proposed control system possesses some robustness properties, allowing for the reduction of velocity overshoot and torque oscillations without extending the transient times. However, the shortcomings of the cascade control structure are still present. The adaptive neural speed controller based on the MRAC approach was implemented in the autonomous model platform [9]. The possibility of autonomous adaptation to changing working conditions is the most crucial advantage of such a structure. After a few adaptation steps, the speed response does not contain overshoots and oscillations. In [16], an adaptive state feedback controller combined with the MRAC approach is proposed for PMSM drive with variable mechanical parameters. The proposed solution ensures high-performance drive operation and robustness against parameter changes. The considered control structure ensures superior load torque compensation. However, the calculation of the initial coefficients is non-trivial.

The synthesis process of MRAC can be divided into the following parts [17]: (i) tuning a stationary controller for initial plant parameters, (ii) developing a reference model with respect to the current system response, (iii) designing an adaptation law for considered variation of plant parameters. The first task is

*e-mail: szczepi@umk.pl

Manuscript submitted 2023-12-13, initially accepted for publication 2024-01-26, published in July 2024.

related to obtaining the desired response of the system. Next, based on this response, the reference model should be created. The last step is responsible for developing the adaptation law to follow the reference model in a plant parameter variation. Selection of the proper model is critical for the accurate operation of the adaptive system, as inaccuracies can result in constant adaptation procedures and unacceptable values of the controller coefficients. In addition, different adaptation mechanisms may be more or less robust to model inaccuracies [8].

This paper considers the selection of a reference model for an adaptive PMSM drive with a state feedback controller (SFC). A PMSM drive with an adaptive state feedback speed controller based on the MRAC approach is proposed and investigated. As depicted earlier, the problem of constant dynamics of the system, regardless of the plant parameters, is considered. The classical Widrow-Hoff rule (W-H) [16] and a relatively new method based on Adaptive Procedure for Optimization Algorithms (APOA) [8] are used in adaptation mechanism. Next, four different reference models regarding control performance and robustness are introduced and analyzed. Extensive simulation tests illustrate the properties of the considered approaches. The preliminary research results describing the above-mentioned concept were presented at the 15th Conference "Sterowanie w Energoelektronice i Napędzie Elektrycznym SENE 2022" [18], while this paper is extended by (i) the experimental verification and (ii) discussion about the impact of adaptation gain on the adaptation process for the different reference models.

The paper is organized as follows. Section 2 describes the state feedback controller for the PMSM drive. Next, the model-reference adaptive control is described in Section 3. The detailed description of the adaptation mechanism based on the W-H rule and APOA is presented in Section 4 and Section 5, respectively. Section 6 describes four different implementations of the reference model that will be examined in a further part of the paper. Simulational and experimental results and in-depth analysis of the proper selection of reference model for MRAC are presented in Section 7 and Section 8, respectively. Finally, Section 9 presents the conclusions.

2. STATE FEEDBACK SPEED CONTROLLER

The synthesis process of the adaptive controller requires a mathematical description of the analyzed plant. In the case of a linearized model of PMSM fed by a voltage source inverter using the feedback linearization method, the mathematical description is as follows [19]:

$$K_p u_{dr}(t) = R_s i_d(t) + L_s \frac{d}{dt} i_d(t), \tag{1}$$

$$K_p u_{qr}(t) = R_s i_q(t) + L_s \frac{d}{dt} i_q(t), \tag{2}$$

$$m_e(t) = K_t i_q(t), \tag{3}$$

$$\frac{d\omega_m(t)}{dt} = \frac{1}{J_m}(m_e(t) - m_o(t) - B_m \omega_m(t)), \tag{4}$$

where: R_s, L_s are resistance and inductance of the PMSM, J_m is moment of inertia, K_t is torque constant, B_m is viscous friction, $i_d(t)$, $i_q(t)$ are current space vector components, $\omega_m(t)$ is angular velocity of the PMSM shaft, K_p is gain of voltage source inverter, $u_{dr}(t)$, $u_{qr}(t)$ are linear components of control voltages, $m_e(t)$ is electromagnetic torque, K_t is torque constant. It should be noted that in the linear voltage formulas described above (equations (1) and (2)) are given by using feedback linearization method based on the following equations:

$$u_{dr}(t) = u_{dn}(t) - u_{do}(t), \tag{5}$$

$$u_{qr}(t) = u_{qn}(t) - u_{qo}(t) \tag{6}$$

with

$$u_{do}(t) = -\frac{L_s p}{K_p} \omega_m(t) i_q(t), \tag{7}$$

$$u_{qo}(t) = \frac{p}{K_p} \omega_m(t) \left[L_s i_d(t) + \psi_f \right], \tag{8}$$

where: p is number pole pairs, and ψ_f is flux linkage.

Next, synthesis of adaptive state feedback speed controller requires knowledge of state space representation, which has the following form [8]:

$$\frac{d\mathbf{x}(t)}{dt} = \mathbf{A}\mathbf{x}(t) + \mathbf{B}\mathbf{u}(t) + \mathbf{F}r(t) \tag{9}$$

with

$$\mathbf{A} = \begin{bmatrix} -\frac{R_s}{L_s} & 0 & 0 & 0 \\ 0 & -\frac{R_s}{L_s} & 0 & 0 \\ 0 & \frac{K_t}{J_m} & -\frac{B_m}{J_m} & 0 \\ 0 & 0 & 1 & 0 \end{bmatrix}, \quad \mathbf{B} = \begin{bmatrix} \frac{K_p}{L_s} & 0 \\ 0 & \frac{K_p}{L_s} \\ 0 & 0 \\ 0 & 0 \end{bmatrix},$$

$$\mathbf{F} = \begin{bmatrix} 0 \\ 0 \\ 0 \\ -1 \end{bmatrix}, \quad \mathbf{x}(t) = \begin{bmatrix} i_d(t) \\ i_q(t) \\ \omega_m(t) \\ x_\omega(t) \end{bmatrix}, \quad \mathbf{u}(t) = \begin{bmatrix} u_{dn}(t) \\ u_{qn}(t) \end{bmatrix},$$

$$r(t) = \omega_m^{\text{ref}}(t),$$

where: $\omega_m^{\text{ref}}(t)$ is reference value of angular velocity, $x_\omega(t)$ is an additional state-space variable that allows ensuring steady-state error-free operation for step changes of reference velocity and load torque [20], and it is defined as follows:

$$x_\omega(t) = \int_0^t \left[\omega_m(\tau) - \omega_m^{\text{ref}}(\tau) \right] \mathrm{d}\tau. \tag{10}$$

The control law for the SFC is defined as

$$\mathbf{u}(t) = -\mathbf{K}\mathbf{x}(t) = -\begin{bmatrix} k_{x1} & k_{x2} & k_{x3} & k_{\omega 1} \\ k_{x4} & k_{x5} & k_{x6} & k_{\omega 2} \end{bmatrix} \mathbf{x}(t), \tag{11}$$

where: k_{x1}–k_{x6} and $k_{\omega 1}$, $k_{\omega 2}$ are gain coefficients of SFC. It is worth pointing out that in the presented model of PMSM drive, angular velocity and d-axis current are independent. Moreover, the d-axis current is unrelated to the q-axis current and angular velocity. In such a case, the k_{x2}, k_{x3}, $k_{\omega 1}$ and k_{x4} coefficients are equal to zero [21,22], and the control law may be simplified to the following formula:

$$\mathbf{u}(t) = -\mathbf{K}\mathbf{x}(t) = -\begin{bmatrix} k_{x1} & 0 & 0 & 0 \\ 0 & k_{x5} & k_{x6} & k_{\omega 2} \end{bmatrix} \mathbf{x}(t). \tag{12}$$

3. MODEL-REFERENCE ADAPTIVE CONTROL FOR PMSM

The principle of the MRAC approach is to keep the system response equal to the reference model response regardless of plant parameters variation or external disturbance [7]. The controller coefficients are adopted to track the desired response, considering the difference between the current angular velocity and the reference model signal. In the case of the adaptive PMSM drive, the d-axis coefficient is constant due to the lack of impact of the d-axis current on the angular velocity. Therefore, only three coefficients (i.e., k_{x5}, k_{x5}, and $k_{\omega 2}$) are adapting to actual operating point. The block diagram of the adaptive PMSM drive system based on the MRAC approach is presented in Fig. 1. The green box highlights the adaptive SFC in the block diagram. The decoupling block is responsible for the realization of the feedback linearization approach (equations (5)–(6)). The orange block, MPAC, corresponds to *a posteriori* model predictive approach for constraints [23], responsible for q-axis current limitation. Moreover, dynamic saturation requires an anti-windup method. For this reason, a method based on back-propagation has been utilized, and it is marked orange on the block diagram. The k_{awu} is the gain of the anti-windup path. Although the q-axis current limitation is possible in the developed control structure, the drive should operate within the linear range of state variables since the MRAC approach aims to keep the same system response regardless of the operating point. In such a case, the drive should operate within a linear range for a considered range of parameter fluctuations (i.e., without limitation of state variables).

4. WIDROW-HOFF RULE

The Widrow-Hoff rule is based on the idea of gradient descent. The adaptation process of the controller coefficient can be written as [16]:

$$\begin{aligned} k_{x5}(n) &= k_{x5}(n-1) + \mu \frac{\partial E}{\partial k_{x5}}, \\ k_{x6}(n) &= k_{x6}(n-1) + \mu \frac{\partial E}{\partial k_{x6}}, \\ k_{\omega 2}(n) &= k_{\omega 2}(n-1) + \mu \frac{\partial E}{\partial k_{\omega 2}}, \end{aligned} \tag{13}$$

where: n is a discrete-time sample, μ is an adaptation gain, and E is a function that is minimizing, which has the following formula:

$$E\left[\mathbf{K}\right] = \frac{1}{2}\left[\omega_m^{MRAC} - \omega_m\right]^2 = \frac{1}{2}e_\omega^2, \tag{14}$$

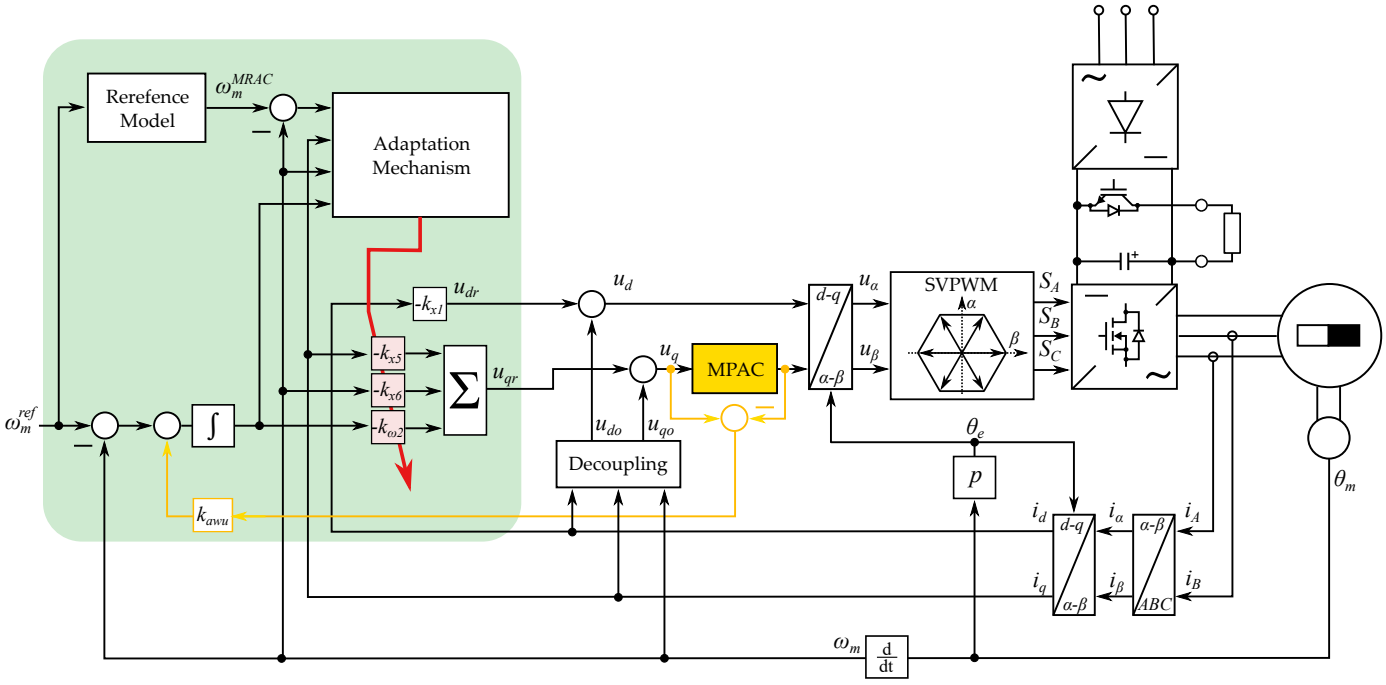

Fig. 1. The block diagram of the adaptive PMSM drive system based on MRAC approach

where: ω_m^{MRAC} is reference model signal. The above-mentioned equations derive the following adaptation rule:

$$\begin{aligned} k_{x5}(n) &= k_{x5}(n-1) - \mu e_\omega(n-1) i_q(n-1), \\ k_{x6}(n) &= k_{x6}(n-1) - \mu e_\omega(n-1) \omega_m(n-1), \\ k_{\omega 2}(n) &= k_{\omega 2}(n-1) - \mu e_\omega(n-1) x_\omega(n-1). \end{aligned} \tag{15}$$

It should be pointed out that the W-H rule updates controller coefficients with sampling frequency. For this reason, it reacts rapidly to plant parameter changes or external disturbance occurrences. On the other hand, the mechanism is sensitive to measurement noises, non-linearities, and improper implementation of the reference model. The last one is related to the fact that providing a reference model that cannot be reached will never stop adaptation. In the actual application, the possible result is that the system will become unstable or even be damaged [7]. A detailed description of the above-mentioned adaptation mechanism can be seen in [16].

5. ADAPTATION PROCEDURE FOR OPTIMIZATION ALGORITHMS

The second adaptation mechanism considered in this paper is based on Adaptation Procedure for Optimization Algorithms [8]. In contrast to the W-H rule, this approach requires a repetitive reference signal and updates controller coefficients at each reference signal period instead of each sampling period. The comparison between these approaches has been presented in Fig. 2 To compare the quality of reference model signal tracking at the entire period of the reference signal, the step-response indicator, which is Integral Absolute Error (IAE), is used. Next, APOA controls the optimization algorithm (e.g., Particle Swarm Optimization, Pattern Search). If the procedure detects that the operating point has been changed, it triggers the optimization of the controller coefficients. If the solution reached is acceptable, it stops the optimization process. The APOA allows the use of most of the optimization algorithms, including nature-inspired ones, which have reached significant attention in many optimization problems [24–27]. However, in this particular case, Pattern Search allows obtaining a relatively short adaptation time and high repeatability of the solution [8]. For this reason, the mentioned algorithm has been selected for optimization and further investigation. The Pattern Search algorithm is an optimization algorithm that examines the neighbor solutions of the current best one to determine the next movement in the search space. These positions are generated by modifying the current position of each dimension by a parameter called step size. If the current position is better than neighbor solutions, the step size is divided by two. The algorithm stops optimization after the step size exceeds the predefined required accuracy. In such a defined adaptation mechanism, the reference model should not significantly impact the solution because the IAE of the entire reference signal period is considered during adaptation. The main disadvantage of this approach is the requirement for a repetitive reference signal. A detailed description of the above-mentioned adaptation mechanism can be seen in [8].

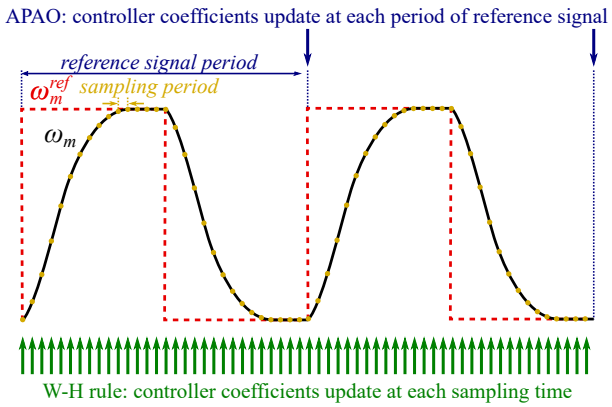

Fig. 2. The comparison of adaptive controller calculation procedure between W-H rule and APOA approach

6. IMPLEMENTATION OF REFERENCE MODEL

To analyze the impact of the proper selection of reference model for adaptive PMSM drive based on the MRAC approach, the following models will be validated:

A: second-order system,
B: first-order system,
C: signal processing based on [16],
D: memory used to archive desired response based on [8].

The first one can be obtained using equations (1)–(4) and equation (12). After Laplace transformation, the following transfer function for the reference model is obtained:

$$G_\omega(s) = \frac{\Omega_m(s)}{\Omega_m^{\text{ref}}(s)} = \frac{a_0}{b_3 s^3 + b_2 s^2 + b_1 s + b_0} \tag{16}$$

with

$$\begin{aligned} a_0 &= b_0 = K_t K_p k_{\omega 2}, \\ b_1 &= B R_s + B K_p k_{x5} + K_t K_p k_{x6}, \\ b_2 &= L_s B + J_{\text{nom}} R_s + J_{\text{nom}} K_p k_{x5}, \\ b_3 &= J_{\text{nom}} L_s. \end{aligned}$$

Using electrical and mechanical time constants (T_e and T_m), and electrical and mechanical static gains(k_e and k_m), equation (16) has been modified to the following form:

$$G_\omega(s) = \frac{a_0^*}{b_3^* s^3 + b_2^* s^2 + b_1^* s + b_0^*} \tag{17}$$

with

$$\begin{aligned} a_0^* &= b_0^* = k_e k_m k_{\omega 2}, \\ b_1^* &= k_e k_{x5} + k_e k_m k_{x6} + 1, \\ b_2^* &= T_e + T_m + T_m k_e k_{x5}, \\ b_3^* &= T_e T_m, \\ T_e &= \frac{L_s}{R_s}, \quad T_m = \frac{J_{\text{nom}}}{B}, \quad k_e = \frac{K_p}{R_s}, \quad k_m = \frac{K_t}{B}. \end{aligned}$$

Due to the enormous difference between the mechanical and electrical time constant ($T_e \ll T_m$), the electrical one is commonly omitted (i.e., $T_e = 0$) [17] with negligible impact to the model response. Therefore, the reference model is simplified to the second-order system:

$$G_\omega^A(s) = \frac{a_0^A}{b_2^A s^2 + b_1^A s + b_0^A} \tag{18}$$

with

$$a_0^A = b_0^A = k_e k_m k_{\omega 2},$$
$$b_1^A = k_e k_{x5} + k_e k_m k_{x6} + 1,$$
$$b_2^A = T_m + T_m k_e k_{x5}.$$

Implementing the above-mentioned second-order system requires precisely defined plant parameters to achieve the same reference model response as the system with initial coefficients response. A first-order system may be considered to provide an option to select a reference model without knowledge of the mathematical description of the plant. In such a case, the time constant is the only parameter present in the equation, and it can be read from the system response or interpreted as a set point of the required dynamic. The first-order system has the following form:

$$G_\omega^B(s) = \frac{1}{\tau^B s + 1}. \tag{19}$$

Implementing the high-order transfer function in microprocessors may provide an issue related to single-precision floating point accuracy. To prevent such a situation, in [16], the authors used a method based on digital filtering of the signals. To achieve the shape of a second-order system, the reference signal is ring-buffered for the last N^C samples. Next, the mean value is calculated, and the low-pass filter is applied. The method uses the following formula to determine the reference model:

$$\omega_m^C(n) = (1 - a^C)\omega_m^C(n-1) + a^C \omega_m^{RB}(n) \tag{20}$$

with

$$\omega_m^{RB}(n) = \frac{1}{N^C} \sum_{i=n-N^C}^{n} \omega_m^{\text{ref}}(i).$$

The last reference model implementation is based on reference signal repeatability. After assuming repeatability, the reference model can be expressed as a memorized system response with an initial controller coefficient and nominal plant parameters. In such a case, knowledge about nominal parameters is not required, and implementation issues are omitted. This method has been proposed in [8].

7. RESULTS

The parameters of the PMSM drive, reference models, and adaptation mechanisms are summarized in Table 1. The reference models responses have been presented in Fig. 3. All models except the first-order system provide similar shapes of the required system response. Models A and D provide the same responses, which are precisely the system response with the nominal plant parameters and initial controller coefficients. The reason is that model A has been directly derived from the mathematical model of PMSM drive (equations (1)–(4), (12)). In the case of model D, the perfect fitness of these responses is guaranteed by the acquisition of the system response, regardless of the system order. A slight difference is presented for reference model C based on

Table 1
The parameters of PMSM drive, reference models and adaptation mechanisms

PMSM drive

Parameter	Value	Parameter	Value
J_{nom}	0.0178 kgm^2	J_{inc}	0.0312 kgm^2
R_s	1.05 Ω	L_s	12.68 mH
K_t	1.1448 Nm/A	B	0.0252 Nms/rad
p	3	K_p	100
f_{PWM}	22 kHz	T_s	45.(45) us

Initial controller coefficients

k_{x1}	0.0725	k_{x5}	0.0900
k_{x6}	0.0979	$k_{\omega 2}$	1.9286

Reference models

a_0^A	8344.1	b_0^A	8344.1
b_1^A	433.1	b_2^A	6.76
τ^B	0.0568		
N^C	704	a^C	0.00123

W-H

μ	$0.25 \cdot T_s$

APOA

$step_{\max}$	10%	$conv_{\text{th}}$	0.01
$alpha$	0.8	Ch_{th}	0.02
$PAAO_{\text{period}}$	30	ChP_{th}	10%

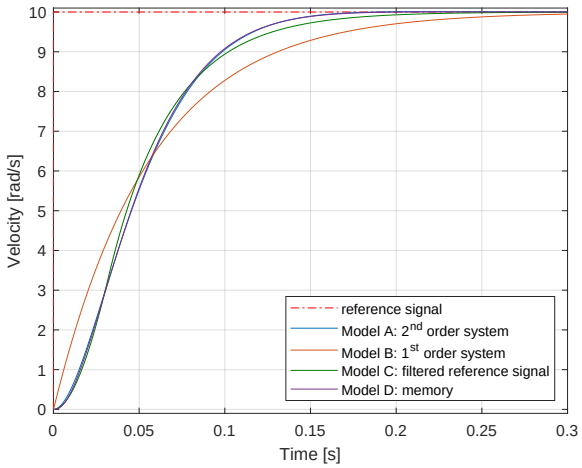

Fig. 3. Comparison of reference models

signal filtering. This approach uses two parameters to fit the required system response. However, the method does not provide the exact shape of a second or third-order system. The shape of the first-order system (model B) is quite different because the model order is inadequate for the system. However, the dynamics are similar to the rest of the models. Although model A provides the best accuracy, the discrete implementation using backward Euler provides the equation with a squared sampling time period (T_s^2). Considering single-precision floating-point calculation, the accuracy is highly dependent on sampling time. The response of model A for sampling frequency ($f_s = 1/T_s$) equal to $0.1, 0.25, 1, 5, 22, 48$ kHz is presented in Fig. 4. It can be seen that the higher sampling frequency provides steady-state error due to the numerical accuracy of single-precision floating-point numbers. On the other hand, the lower sampling frequency provides poor accuracy at transient states. Therefore, properly selecting sampling frequency during the generation of reference model A is crucial for adequately operating adjustment mechanisms. The sampling frequency equal to $f_s = 1$ kHz was selected in this case. Finally, it should be noted that the sampling frequency of reference model generation is not equal to the sampling frequency of the control loop. Another possibility for solving the issue related to the accuracy of single-precision floating-point numbers is to use a different time unit than the SI, i.e., milliseconds instead of seconds. In such a case, the squared sampling time period will be in the range of floating point precision, and the accuracy of the model response will be increased. However, such an approach requires user experience to determine the time unit required for proper microprocessor systems calculations.

The evaluation was as follows: the moment of inertia changes at 5 s from J_{init} to J_{inc}, and the torque load with 1 Nm is applied at 30 s. Due to that, the paper is related to the selection of reference model, and only the final fitness is presented for each adaptation mechanism and reference model implementation. In addition, the IAE and controller coefficients in the time domain are presented to indicate the difference in adaptation behavior. The angular velocity, q-axis current, and a control signal for the last period of the reference signal are presented in Fig. 5, and the IAE and controller coefficients in the time domain are presented in Fig. 6. From the step responses, one can see that APOA provides oscillation-free operation for all implemented models. Also, the implementation of a first-order system provides a smooth angular velocity response. It noticeably differs from the rest of the results. However, the desired shape of the system response is kept similar to the initial one, i.e., no oscillation, no overshoot, and close to the desired rise time. It is worth pointing out that APOA triggers optimization just after the moment of inertia has been changed and finishes adaptation within around 10 seconds. The step change of torque load has triggered only for model A. However, the obtained solution for the next evaluated coefficients provides an acceptable response, and APOA has stopped the optimization. One can see that changes in controller coefficients change every 1 second, and only one value changes at once. It is related to the application of the Pattern Search algorithm for optimization. Finally, regardless of the implemented reference model, APOA has found the solution with an IAE value close to the initial one (i.e., IAE value for a nominal moment of inertia and initial controller coefficients). In the case of the W-H rule, the first-order system (B) used as the reference model provides significant oscillations in steady-state for non-zero reference value. Moreover, the reference model based on signal filtering (C) also has noticeable oscillations at the rising edge of the angular velocity. Small oscillations are also present for models A and D. However, they are caused by relatively high adaptation gain and have a negligible impact on angular velocity response. The IAE plot shows that the W-H rule tries to adapt to models B and C until the moment of inertia has been changed. The reason is that these reference models differ from the system initial response (see Fig. 3). The W-H rule provides a high final IAE value for the reference model based on the first-order system (B). For the signal filtering-based reference

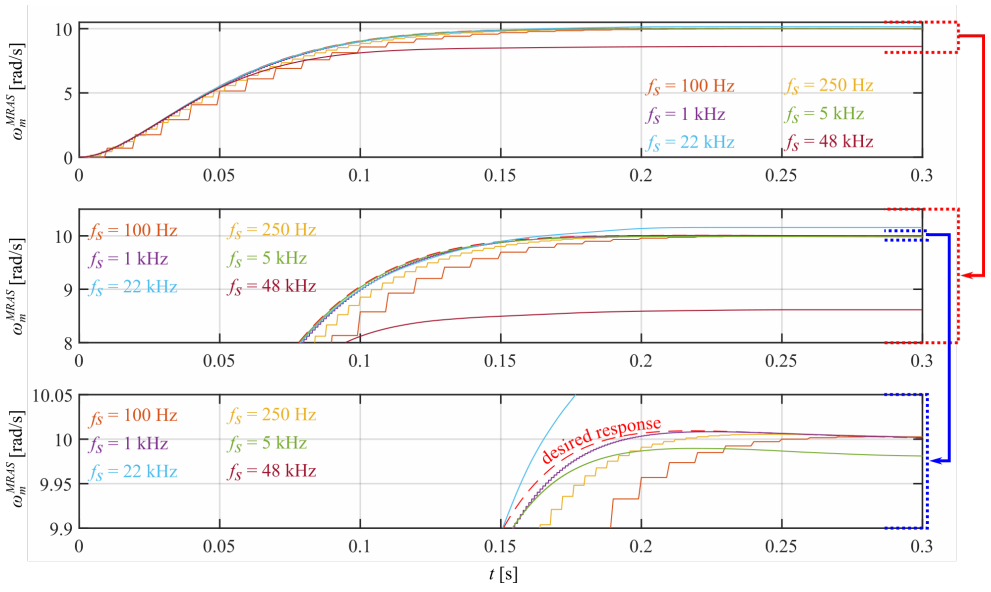

Fig. 4. Comparison of reference model A responses calculated with different sampling frequencies

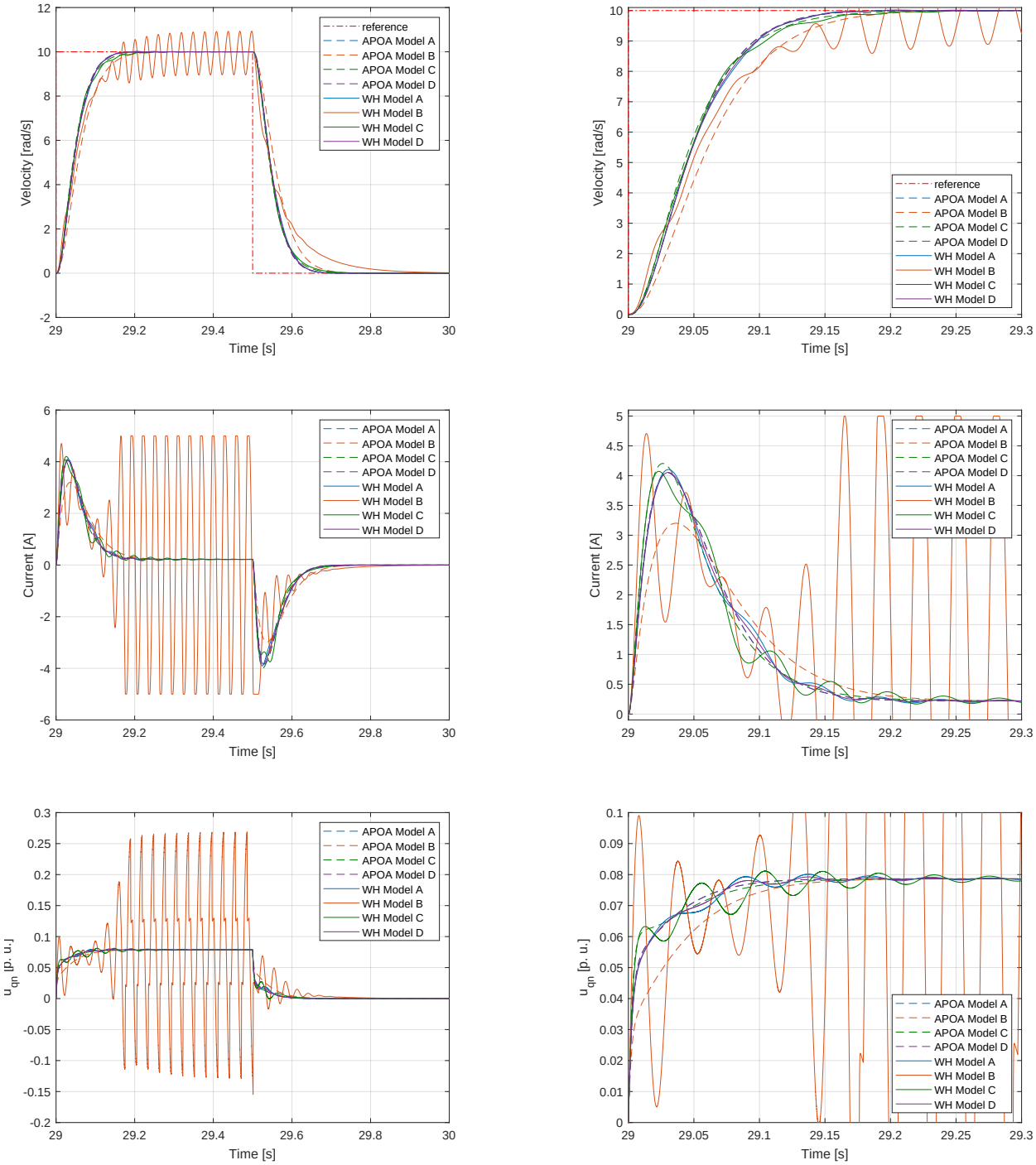

Fig. 5. Angular velocity, q-axis current, and q-axis control signal obtained for adaptation mechanism based on W-H rule and APOA with four different model reference implementations. Left column: entire signal reference period, right column: zoom in on the rising edge

model (C), the IAE has a similar value to the rest of the results. However, it has the highest value.

Next, the same experiment has been evaluated for the current limitation to 3 A to present the behavior of the adaptation mechanism in the case of the non-reachable reference model. After increasing the moment of inertia, the current limitation causes the same dynamic as the initial response is impossible to reach. The angular velocity, q-axis current, and a control signal for the last period of the reference signal are presented in Fig. 8, and the IAE and controller coefficients in the time domain are presented in Fig. 7. One can see that all results for the W-H rule provide oscillating characteristics in step responses. Moreover, the final IAE values are very high. In the case of APOA, the adaptation process required significantly more time since the stop criteria are related to reaching satisfactory fitness to the reference model, which is impossible in this experiment.

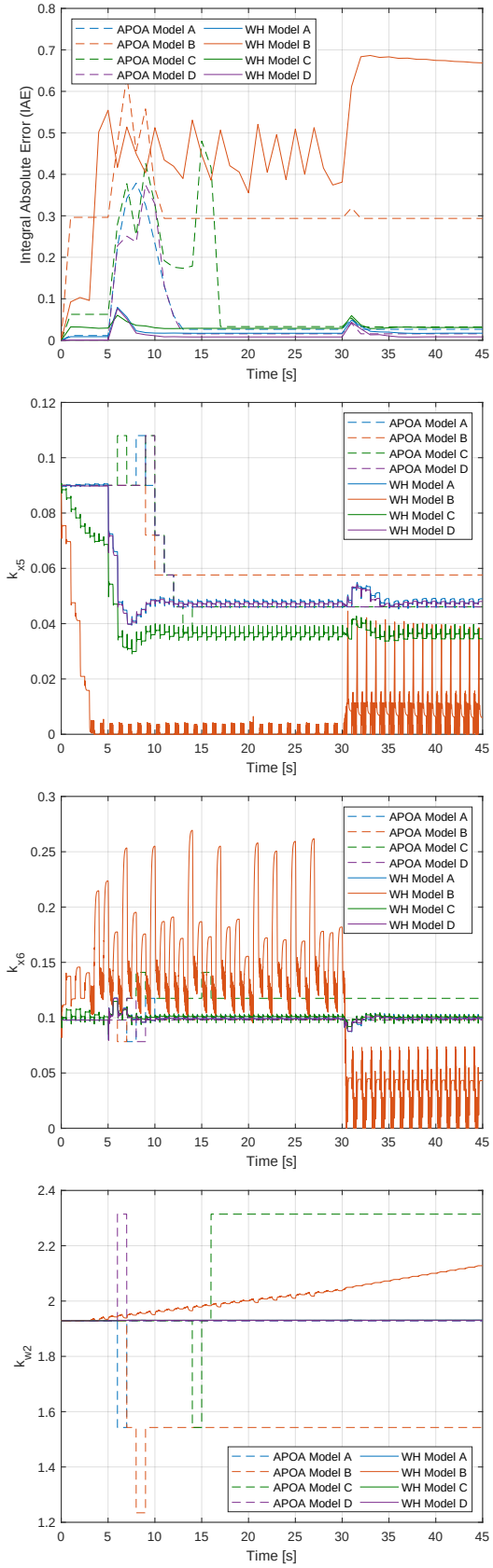

Fig. 6. Integral absolute error indicator and controller coefficients in time domain obtained for adaptation mechanism based on W-H rule and APOA with four different model reference implementations

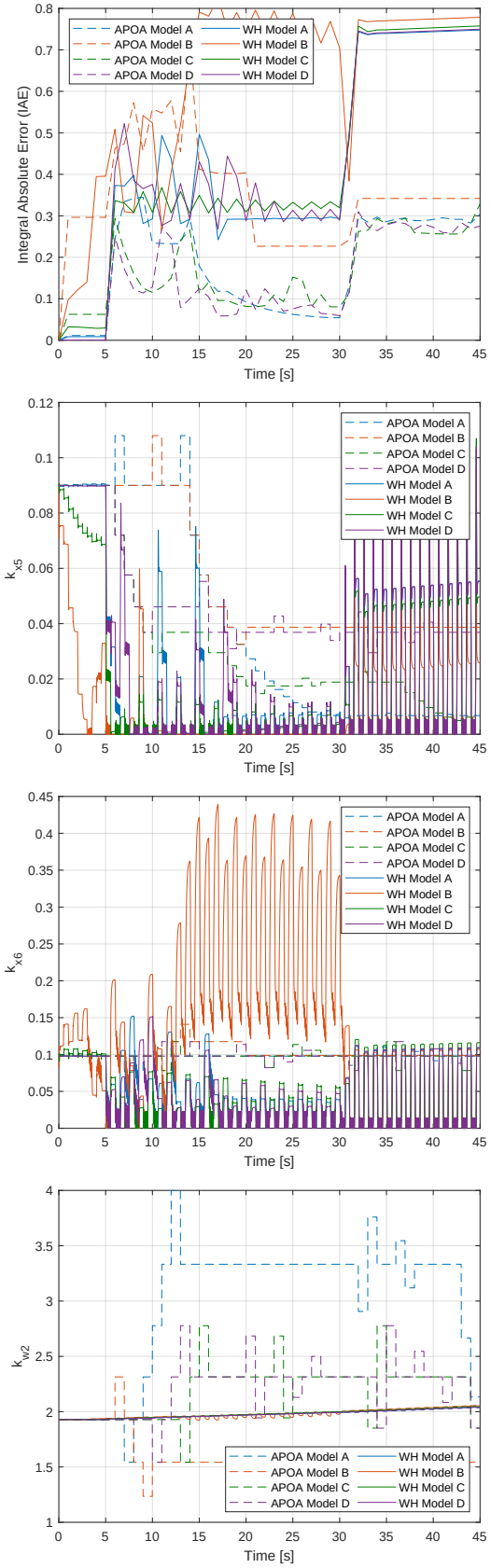

Fig. 7. Integral absolute error indicator and controller coefficients in time domain obtained for adaptation mechanism based on W-H rule and APOA with four different model reference implementations. Operation under current limitation

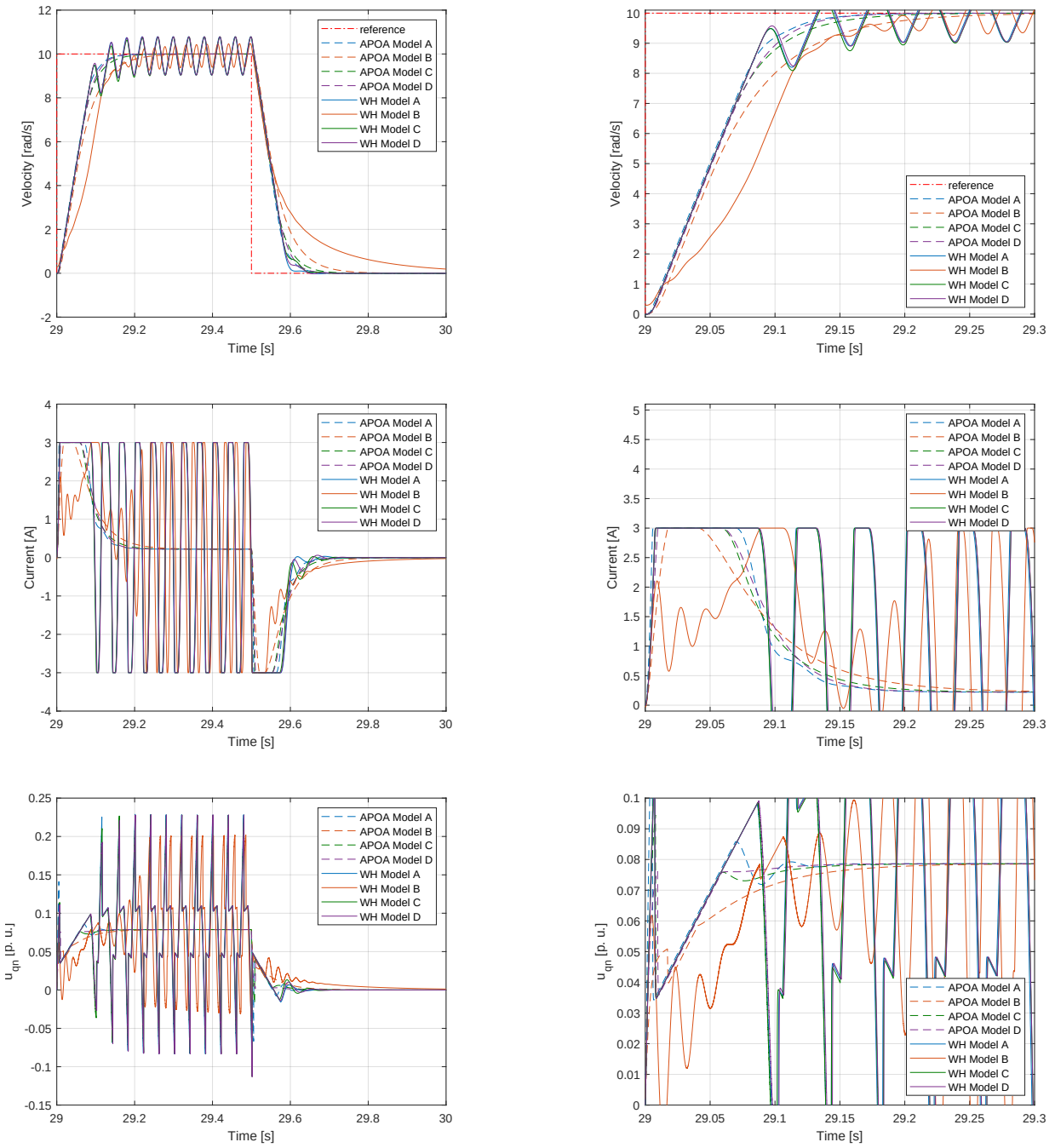

Fig. 8. Angular velocity, q-axis current, and q-axis control signal obtained for adaptation mechanism based on W-H rule and APOA with four different model reference implementations. Operation under current limitation to 3 A. Left column: entire signal reference period, right column: zoom in on the rising edge

The second stop criterion is the convergence of the optimization algorithm, which takes some time. However, from the current responses, one can see that all APOA examinations with different reference models provide oscillation-free operation. The IAE value is significantly lower than solutions obtained by the W-H rule.

The additional simulation examinations were conducted to provide information on the highest possible adaptation gain (μ) for the W-H rule that results in smooth angular speed, currents, and control signal waveforms. The procedure was as follows: (i) start with adaptation gain equal to the $0.25 \cdot T_s$, which has been used in the above experiments, and (ii) decrease it until the above-mentioned condition has been satisfied. The results of reference models A (second order system) and D (memory) are the same: smooth operation and the shortest adaptation time were obtained for $\mu = 0.10 \cdot T_s$. In comparison, the reference model C (signal filtering) has value $\mu = 0.06 \cdot T_s$. The adaptation time was around 13 and 15 seconds for reference models A/D and C,

respectively. These values should be interpreted as demonstration values because the selection of the adaptation gain was based on the Author's subjective opinion about the smoothness of waveforms. However, the higher accuracy of reference model selection allows for a significantly reduced adaptation time, providing a similar final response of the system. In the case of reference model B (first order system), the satisfaction of smooth angular speed and current waveforms was impossible to reach with adaptation time less or equal to 100 seconds. In the Authors' opinion, such a long adaptation time declassifies the application of the reference model for the W-H rule.

8. EXPERIMENTAL VERIFICATION

The photo of the laboratory stand is presented in Fig. 9. The most important parts are: (i) 2.76 kW PMSM motor, (ii) prototype VSI with SiC power devices (Cree 300CCS020M12CM2) with dedicated six-channel gate driver (Cree CGD15FB45P1) was used to supply the PMSM, (iii) STM32F407VGT6 microcontroller with ARM Cortex-M4 core, (iv) auxiliary PMSM supplied by commercial drive (Kollmorgen AKD-P00307-NBCC-E000), and (v) mechatronic device responsible for the moment of inertia variations. Due to the unmodelled nonlinearities of the PMSM model and potential parameters mismatch with the real laboratory stand, the coefficient of the adaptation gain for the W-H rule was reduced to $0.05 \cdot T_s$ to obtain the smooth waveforms. For the APOA, the parameters were the same as used in the simulation verification.

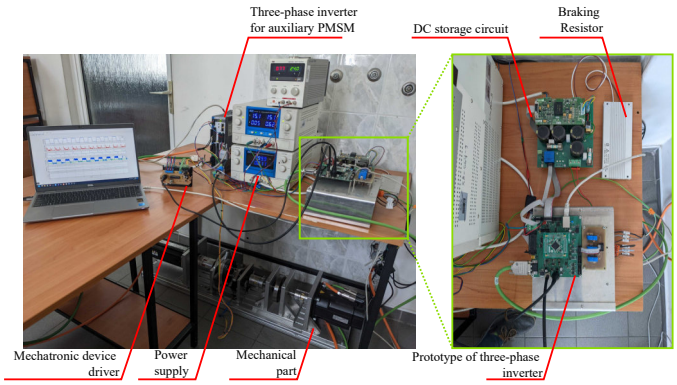

Fig. 9. Laboratory stand

The experiments were conducted as follows:

- second-order system has been implemented, due to the best performance of the adaptation process,
- moment of inertia increases ($J_{\text{nom}} \rightarrow J_{\text{inc}}$) in first second of experiment,
- torque load (1 Nm) was applied at 20.25 s,
- torque load was decreased to 0 Nm at 40.25 s,
- current limitation was not used.

The obtained results in the form of angular velocity, d- and q-axis currents, and d- and q-axis control signals are presented in Fig. 10 and Fig. 11 for W-H rule and APOA, respectively.

The obtained experimental results prove that the reference model has been properly selected. The experimental results are consistent with the simulation. Both adaptation mechanisms successfully reduce the overshot after the moment of inertia increases. Proper selection of reference model allowed for providing oscillation-free waveforms. Moreover, the analyzed control structures are robust to the applied load torque.

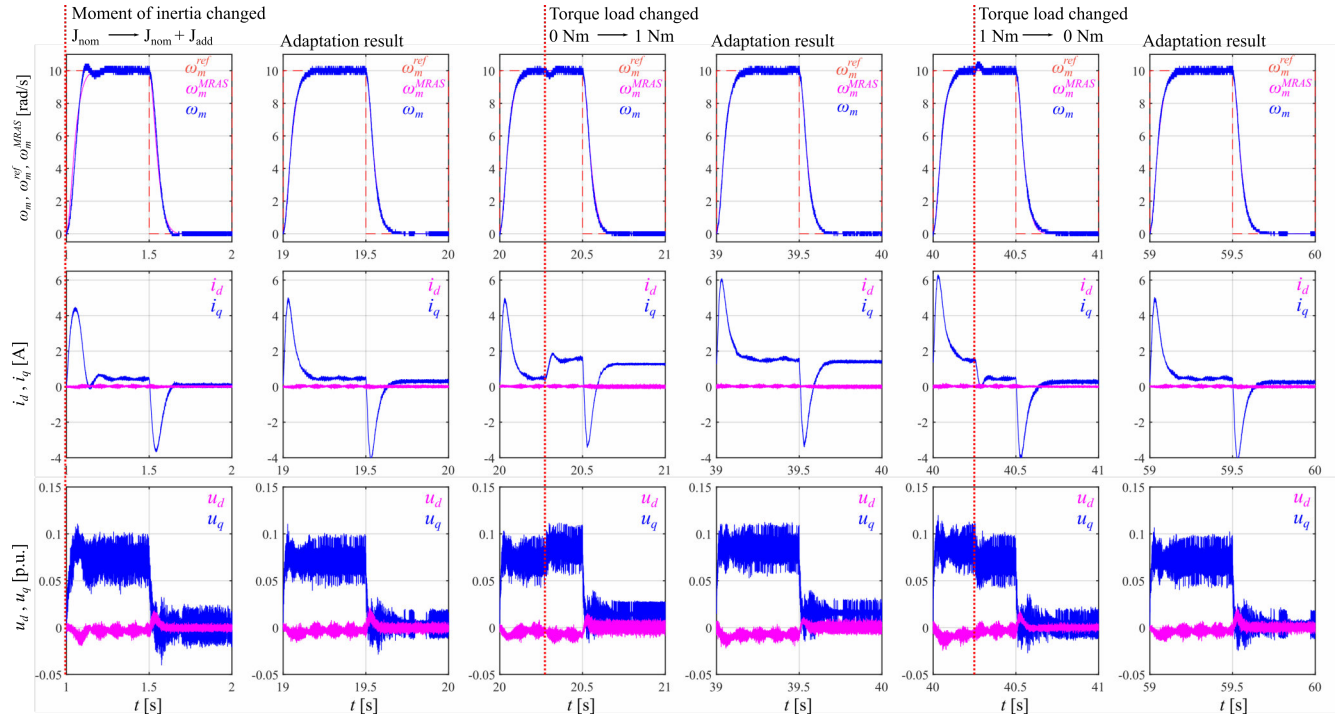

Fig. 10. Experimental results in the form of angular velocity, d- and q-axis currents, and d- and q-axis control signals obtained for the adaptation mechanism based on W-H rule and reference model implemented as a second-order system.

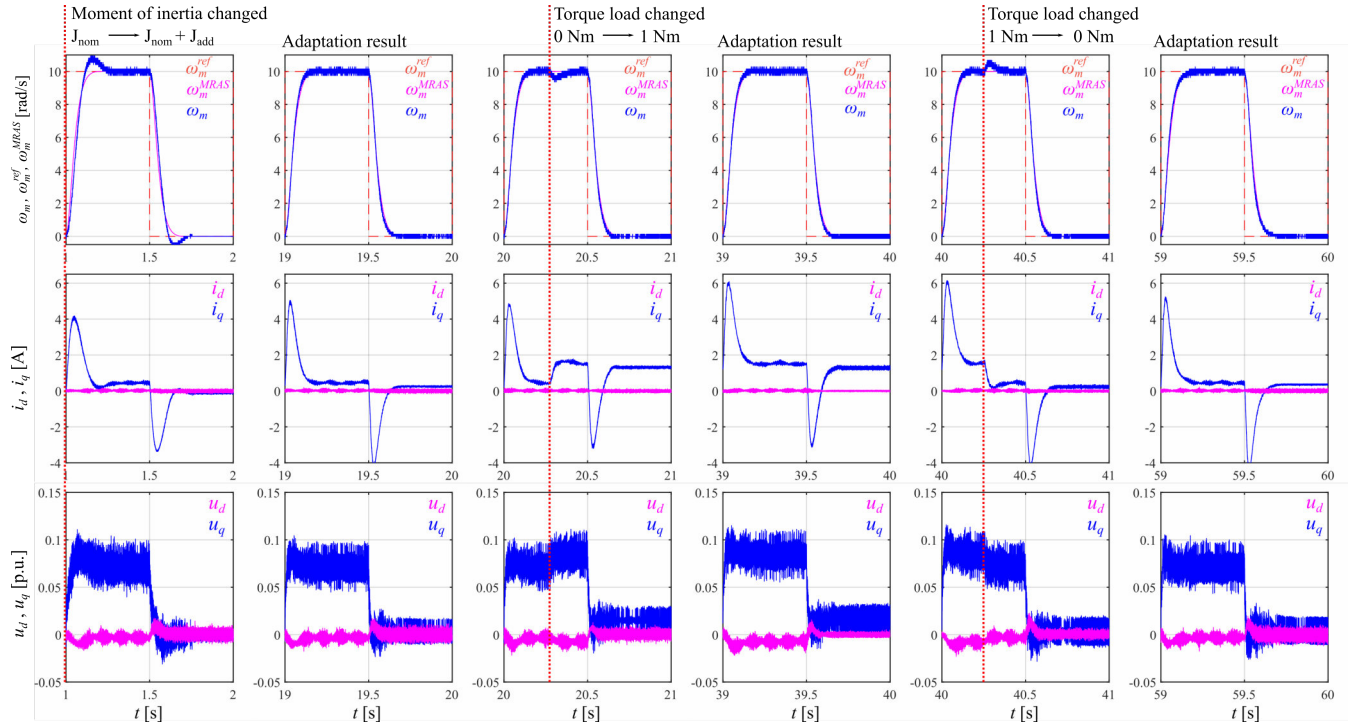

Fig. 11. Experimental results in the form of angular velocity, d- and q-axis currents, and d- and q-axis control signals obtained for the adaptation mechanism based on APOA and reference model implemented as a second-order system.

9. CONCLUSION

This paper investigates the selection of a reference model for MRAC application in PMSM drive. Four different implementations of the reference model were proposed: (A) based on the mathematical model of the plant (second-order system), (B) first-order system, (C) reference signal filtering, and (D) memory-based solution for repetitive processes. Also, two adaptation mechanisms were utilized: the W-H rule and the APOA. The results proved that the W-H rule requires a reference model that accurately imitates the system response. Even slight differences in nominal system response (i.e., nominal plant parameters and initial controller coefficients) and reference model response provide noticeable oscillations in angular velocity. To prevent it, the adaptation gain has to be decreased. However, such an action will increase the time required for adaptation to the new operating point of the system.

In the case of APOA, the reference model implementation does not have such a significant impact. All experiments prove that APOA is robust against inaccurate reference model implementation. The final results were free of oscillations for each case, and the general characteristics were achieved.

The proper selection of the reference model significantly impacts adaptive system response. An inaccurate model may increase the adaptation time due to the requirement to reduce adaptation gain. In a critical case, improper selection of reference model may provide oscillations of the system, which is unacceptable. On the other hand, selecting a more advanced adaptation mechanism may minimize the impact of the inaccurate selection of the reference model.

REFERENCES

[1] V. Koropouli, A. Gusrialdi, S. Hirche, and D. Lee, "An extremum-seeking control approach for constrained robotic motion tasks," *Control Eng. Pract.*, vol. 52, pp. 1–14, 2016.

[2] T. Tarczewski, Ł.J. Niewiara, and L.M. Grzesiak, "Artificial neural network-based gain-scheduled state feedback speed controller for synchronous reluctance motor," *Power Electron. Drives*, vol. 6, 2021.

[3] M. Korzonek, G. Tarchala, and T. Orlowska-Kowalska, "A review on mras-type speed estimators for reliable and efficient induction motor drives," *ISA Trans.*, vol. 93, pp. 1–13, 2019.

[4] X. Wang, B. Ufnalski, and L.M. Grzesiak, "Adaptive speed control in the pmsm drive for a non-stationary repetitive process using particle swarms," in *2016 10th International Conference on Compatibility, Power Electronics and Power Engineering (CPE-POWERENG)*. IEEE, 2016, pp. 464–471.

[5] E. Kilic, H.R. Ozcalik, and S. Yilmaz, "Efficient speed control of induction motor using rbf based model reference adaptive control method," *Automatika: Časopis za Automatiku, Mjerenje, Elektroniku, Računarstvo i komunikacije*, vol. 57, no. 3, pp. 714–723, 2016.

[6] Z.A. Alrowaili *et al.*, "Robust adaptive hcs mppt algorithm-based wind generation system using model reference adaptive control," *Sensors*, vol. 21, no. 15, p. 5187, 2021.

[7] K.J. Åström and B. Wittenmark, *Adaptive control*. Courier Corporation, 2013.

[8] R. Szczepanski, T. Tarczewski, and L.M. Grzesiak, "Application of optimization algorithms to adaptive motion control for repetitive process," *ISA Trans.*, vol. 115, pp. 192–205, 2021.

[9] M. Malarczyk, J.-R. Tapamo, and M. Kaminski, "Application of neural data processing in autonomous model platform—a com-

plex review of solutions, design and implementation," *Energies*, vol. 15, no. 13, p. 4766, 2022.

[10] J.C. Travieso-Torres and M.A. Duarte-Mermoud, "Normalized model reference adaptive control applied to high starting torque scalar control scheme for induction motors," *Energies*, vol. 15, no. 10, p. 3606, 2022.

[11] H.H. Nguyen, M.T. Tran, D.H. Kim, H.K. Kim, and S.B. Kim, "Velocity controller design for fish sorting belt conveyor system using m-mrac and projection operator," *J. Power Syst. Eng.*, vol. 21, no. 4, pp. 42–50, 2017.

[12] H. Liu, X. Zhang, Y. Chen, M. Taha, and H. Xu, "Active damping of driveline vibration in power-split hybrid vehicles based on model reference control," *Control Eng. Pract.*, vol. 91, p. 104085, 2019.

[13] E. Arabi and T. Yucelen, "A set-theoretic model reference adaptive control architecture with dead-zone effect," *Control Eng. Pract.*, vol. 89, pp. 12–29, 2019.

[14] X. Sun, Y. Zhang, X. Tian, J. Cao, and J. Zhu, "Speed sensorless control for ipmsms using a modified mras with gray wolf optimization algorithm," *IEEE Trans. Transp. Electrif.*, vol. 8, no. 1, pp. 1326–1337, 2021.

[15] M. Öztekin, O. Kiselychnyk, and J. Wang, "Nonlinear optimal control for interior permanent magnet synchronous motor drives," in *2022 European Control Conference (ECC)*. IEEE, 2022, pp. 590–595.

[16] R. Szczepanski, T. Tarczewski, and L. Grzesiak, "Pmsm drive with adaptive state feedback speed controller," *Bull. Pol. Acad. Sci. Tech. Sci.*, vol. 68, no. 5, 2020.

[17] M. Kamiński, "Zastosowanie algorytmu bat w optymalizacji obliczeń adaptacyjnego regulatora stanu układu dwumasowego," *Przegląd Elektrotechniczny*, vol. 93, no. 1, pp. 300–304, 2017, in Polish.

[18] R. Szczepanski, T. Tarczewski, and L.M. Grzesiak, "Wybór modelu odniesienia dla adaptacyjnego napędu z silnikiem PMSM bazującego na metodzie MRAC," in *Procedings of conference Sterowanie w Energoelektronice i Napedzie Elektrycznym SENE 2022*, 2022, in Polish.

[19] L.M. Grzesiak and T. Tarczewski, "Pmsm servo-drive control system with a state feedback and a load torque feedforward compensation," *COMPEL-Int. J. Comput. Math. Electr. Electron. Eng.*, vol. 32, no. 1, pp. 364–382, 2013.

[20] G.F. Franklin *et al.*, *Digital control of dynamic systems*. Addison-Wesley Reading, MA, 1998, vol. 3.

[21] X. Sun, C. Hu, G. Lei, Y. Guo, and J. Zhu, "State feedback control for a pm hub motor based on gray wolf optimization algorithm," *IEEE Trans. Power Electron.*, vol. 35, no. 1, pp. 1136–1146, 2019.

[22] J. Cao, X. Sun, and X. Tian, "Optimal control strategy of state feedback control for surface-mounted pmsm drives based on auto-tuning of seeker optimization algorithm," *Int. J. Appl. Electromagn. Mech.*, vol. 66, no. 4, pp. 705–725, 2021.

[23] T. Tarczewski and L.M. Grzesiak, "Constrained state feedback speed control of pmsm based on model predictive approach," *IEEE Trans. Ind. Electron.*, vol. 63, no. 6, pp. 3867–3875, 2015.

[24] A.F.U. Din *et al.*, "Robust flight control system design of a fixed wing uav using optimal dynamic programming," *Soft Comput.*, pp. 1–12, 2022.

[25] M. Dehghani, Š. Hubálovskỳ, and P. Trojovskỳ, "Cat and mouse based optimizer: a new nature-inspired optimization algorithm," *Sensors*, vol. 21, no. 15, p. 5214, 2021.

[26] F. Gul *et al.*, "A centralized strategy for multi-agent exploration," *IEEE Access*, vol. 10, pp. 126 871–126 884, 2022.

[27] F. Gul, W. Rahiman, S. Alhady, A. Ali, I. Mir, and A. Jalil, "Meta-heuristic approach for solving multi-objective path planning for autonomous guided robot using pso–gwo optimization algorithm with evolutionary programming," *J. Ambient Intell. Humaniz. Comput.*, vol. 12, pp. 7873–7890, 2021.